ACS APPLIED MATERIALS & INTERFACES

RESEARCH ARTICLE

www.acsami.org

# Light Sensing in a Photoresponsive, Organic-Based Complementary Inverter

Sungyoung Kim,[†] Taehoon Lim,[†] Kyoseung Sim,[†] Hyojoong Kim,[†] Youngill Choi,[†] Keechan Park,[‡] and Seungmoon Pyo*[,†]

[†]Department of Chemistry and [‡]Department of Electronic Engineering, Konkuk University, 1 Hwayang-dong, Kwangjin-Gu, Seoul, 143-701, Korea

**ABSTRACT:** A photoresponsive organic complementary inverter was fabricated and its light sensing characteristics was studied. An organic circuit was fabricated by integrating *p*-channel pentacene and *n*-channel copper hexadecafluorophthalocyanine (F16CuPc) organic thin-film transistors (OTFTs) with a polymeric gate dielectric. The F16CuPc OTFT showed typical *n*-type characteristics and a strong photoresponse under illumination. Whereas under illumination, the pentacene OTFT showed a relatively weak photoresponse with typical p-type characteristics. The characteristics of the organic electro-optical circuit could be controlled by the incident light intensity, a gate bias, or both. The logic threshold ($V_M$, when $V_{IN} = V_{OUT}$) was reduced from 28.6 V without illumination to 19.9 V at 6.94 mW/cm$^2$. By using solely optical or a combination of optical and electrical pulse signals, light sensing was demonstrated in this type of organic circuit, suggesting that the circuit can be potentially used in various optoelectronic applications, including optical sensors, photodetectors and electro-optical transceivers.

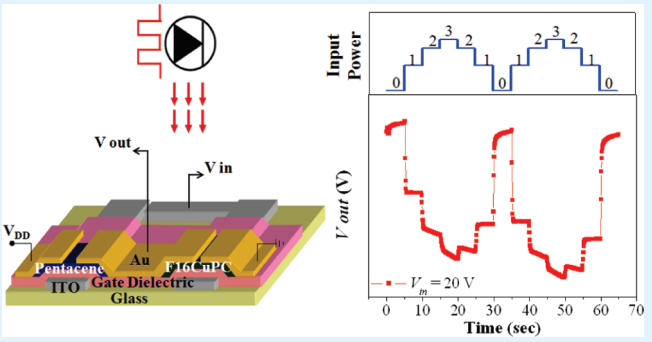


**KEYWORDS:** optical sensor, organic thin-film transistor, phototransistor, complementary inverter, photoresponse, organic semiconductor

## INTRODUCTION

The electrical performance of organic optoelectronic devices, such as organic thin-film transistors (OTFTs),[1−12] organic solar cells,[13,14] and light-emitting diodes,[14] has been improved considerably. Of such devices, OTFTs receive much research interest. Organic semiconductors offer many advantages over their inorganic counterparts including their lighter weight, low-temperature processing, large-area coverage, mechanical flexibility and low-cost processing. High performance OTFTs based on various organic semiconductors and dielectrics have been reported,[1] with field-effect charge carrier mobilities of up to 6.3 and 5.3 cm$^2$/V.s for recently reported p- and n-type OTFTs, respectively.[2] Those organic semiconductors include pentacene,[1,2] solution-processed functionalized pentacene,[3] perylene derivative,[4] $C_{60}$,[2] pyrazine derivative,[5] and copperhexadecafluorophthalocyanine (F16CuPC).[6,7] In addition, high performance OTFTs can be used to fabricate organic complementary inverters, a basic component of integrated circuits.[8−12]

Organic phototransistors (OPTs) are three terminal organic devices where light can be used as an external trigger for the operation of the OTFT along with the conventional electrodes: source, drain, and gate because incident photons with energy of at least the semiconductor's band gap can generate additional charge carriers in the channel region.[15,16] OPTs are attractive for application in such as photodetectors and photoswitches because of their large absorption and efficient photocurrent generation under ultraviolet−visible illumination. Therefore, efficient charge transport in OPTs can be achieved through the combination of gate bias and incident light intensity.[15−20] The unique advantage of OPTs is that they can integrate the switching ability of a transistor with light detection in a single device and hence eliminate the need for additional processing steps. In addition, OPTs can be fabricated by relatively easy and inexpensive processes at low processing temperatures. Such OPTs can also be applied in the fabrication of organic circuits, forming efficient photodetectors and photoswitches, controllable through the gate bias and light intensity.[21,22]

This work reports a photoresponsive organic circuit based on OPTs with organic semiconductors and polymer gate dielectric. For this, *n*-channel copperhexadecafluorophthalocyanine (F16CuPC) and *p*-channel pentacene were employed as active layers because they are relatively stable in air and have good charge carrier transport characteristics.[1,2,6,7] Polymeric gate dielectric, cross-linked poly(vinylphenol), was employed instead of rigid, expensive inorganic dielectrics that require high temperatures fabrication processes, and so could be suitable for realizing low-cost, flexible optoelectronic devices. OPTs based on F16CuPC have been reported earlier. Our group reported OPTs with F16CuPc thermally evaporated thin-film and polymeric gate

**Received:** December 30, 2010
**Accepted:** March 15, 2011
**Published:** March 15, 2011

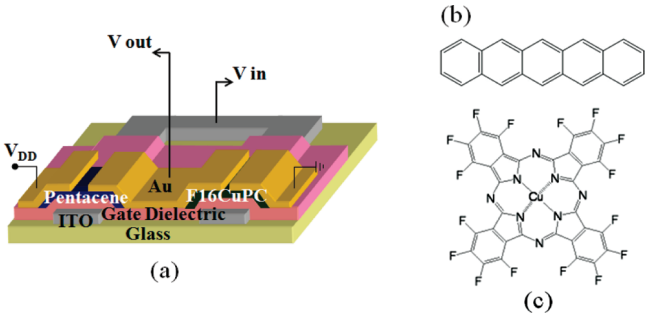


**Figure 1.** (a) Complementary inverter. Chemical structures of (b) pentacene and (c) hexadecafluorophthalocyanine (F16CuPc).

dielectric[15,16] and Tang et al. reported OPT with F16CuPc single-crystalline submicro/nanometer ribbon and silicon dioxide gate dielectric with high performance and discussed well the photoresponse behavior of F16CuPc-based OPT.[23] OPTs based on pentacene with silicon dioxide or polymeric gate dielectric also have been reported by some groups.[24] It is worthwhile to mention that the performance of the devices reported by them is somewhat different each other and cannot be directly compared because device structure geometry, type of gate dielectric used and measurement conditions are not the same. In this study we report the fabrication of photosensitive organic complementary inverter based on F16CuPc, pentacene, and polymeric gate dielectric and its dynamic photoresponses and light sensing characteristics.

## EXPERIMENTAL SECTION

Organic semiconductors, copperhexadecafluorophthalocyanine (F16CuPC), and pentacene were purchased from Aldrich and used as received. Indium tin oxide (ITO) coated glass was used as a substrate and gate electrode. It was patterned by a photolithographic method and cleaned sequentially in an ultrasonic bath with detergent, deionized water, acetone, and isopropyl alcohol each for 15 min. Cross-linked PVP (CL-PVP) precursor solution was prepared by mixing poly(4-vinylphenol) (PVP) (10 wt %) with a cross-linking agent, poly(melamine-co-formaldehyde) (5 wt %) and propylene glycol monomethyl ether acetate (PGMEA) (85 wt %). The solution was spin-coated on to the gate electrodes and soft-baked at 60 °C for 5 min on a hot plate in ambient conditions and hard-baked at 175 °C for 1 h in a vacuum oven ($10^{-3}$ Torr). The final thickness of the dielectric layer was controlled to be ~450 nm. Dynamic photoresponse was measured when cross-linked PVP (CL-PVP) gate dielectric was employed. Pentacene and F16CuPc were vacuum-deposited next to each layer at a base pressure of $5 \times 10^{-6}$ Torr through a shadow mask on the gate dielectric. The deposition rate and substrate temperature were 0.3 Å/s and 90 °C for pentacene, and 0.1 Å/s and 25 °C for F16CuPc, respectively. The thicknesses of pentacene and F16CuPc were controlled to be ~50 and 35 nm, respectively. Finally, the organic inverter was completed by thermally evaporating 35 nm thick gold electrodes using a shadow mask on the active layer to form the source and drain electrodes (Figure 1a). The channel lengths and widths were 250 and 200 $\mu$m for the *p*-channel OTFTs and 50 and 4000 $\mu$m for the *n*-channel OTFT, respectively. The thickness of dielectric layer was measured using an AMBIOS XP-100 surface profiler. OTFTs' electrical characterization and were performed using an HP4145B semiconductor parameter analyzer controlled by LabView program. All electrical measurements were performed in ambient conditions. For the characterization of the devices under illumination, a common incandescent lamp was used as a light source and the intensity was measured in situ using a light meter. Dynamic photoresponses of the inverter were measured by exposing the device to the light source using a mechanical shutter.

## RESULTS AND DISCUSSION

Figure 1a shows the structure of the organic complementary inverter, which comprised *n*-channel and *p*-channel OTFTs. Chemical structures of the organic semiconductors, pentacene for the *p*-type OTFT and copperhexadecafluorophthalocyanine (F16CuPC) for the *n*-type OTFT are shown in Figure 1b and c, respectively. Each OTFT had bottom gate and top-contact geometries.

The performance of pentacene based OTFTs[1] has been reported to be much better than that of F16CuPc based OTFTs:[6] in direct comparisons that had similar channel lengths ($L$) and widths ($W$), the on-state current of pentacene OTFTs was usually larger than that of F16CuPc OTFTs at fixed gate and drain voltages. For the fabrication of high performance complementary inverter based on *n*- and *p*-channel OTFTs, it is necessary to match the performance of each OTFT. $V_{out}$ of an ideal inverter intersects $V_{dd}/2$ when $V_{in}$ is equal to $V_{dd}/2$. This requires that same drain current should flow through *n*- and *p*-channel OTFT from $V_{dd}$ to GND when the magnitudes of $V_{gs}$ and $V_{ds}$ are same as $V_{dd}/2$ for both *n*- and *p*-channel OTFT. To meet this condition, the device geometry should be modified considering other parameters, such as mobility and current level.[12,22] Therefore, in this study, to match the on-state current of each OTFT its channel length ($L$) and width ($W$) was intentionally controlled. These were 250 and 200 $\mu$m for the *p*-channel OTFT and 50 $\mu$m and 4,000 $\mu$m for the *n*-channel OTFT, respectively. Figure 2a shows output characteristic (drain current vs drain voltage, $I_{ds}$ vs $V_{ds}$) curves of the pentacene and F16CuPc OTFT in the complementary inverter. Although the sizes of the OTFTs were carefully controlled, on-state current in pentacene OTFT is still higher than that of F16CuPc OTFT. The currents were not matched perfectly because the length of the *n*-channel OTFT could not be reduced further due to limitations of the fabrication facility. Typical *p*-channel (dominant hole transport) and *n*- channel (dominant electron transport) characteristics with a clear transition from linear to saturation regions were observed in both OTFTs. That is, at a specified $V_{gs}$, $I_{ds}$ increased initially linearly with increasing voltage in the low voltage region before saturating in the high voltage region. The transfer characteristic (drain current vs gate voltage, $I_{ds}$ vs $V_{gs}$) curves of the same OTFTs are shown in Figure 2b. At $V_{ds} = -40$ V, the pentacene OTFT had a field−effect mobility of 0.15 $cm^2$/V.s, a threshold voltage of −10 V and a subthreshold swing (ss) of 2.6 V/dec The values for the F16CuPc OTFT at $V_{ds} = 40$ V, were $6.1 \times 10^{-4}$ $cm^2$/V.s, 14 and 2.1 V/dec, respectively.

To investigate the photoresponses of the pentacene and F16CuPC OTFTs in a complementary inverter with cross-linked PVP gate dielectric, each OTFT was exposed to white light separately. Figure 3 shows their photoresponses with respect to illumination. The dynamic photoresponse of the devices was studied by measuring the drain current of each OTFT as a function of time during repeated switching of the light using a mechanical shutter. The responses of the devices were measured under constant $V_{ds} = V_{gs} = -10$ V for the pentacene OTFT and $V_{ds} = V_{gs} = 10$ V for the F16CuPC OTFT. During the test, light with power of 6.94 mW/$cm^2$ was repeatedly turned on for 10 s and then off for 20 s. While a large increase in drain current was observed in the F16CuPC OTFT during illumination, little change in drain current was observed in the pentacene OTFT. When the light was turned off, the current decreased to the dark current level almost immediately.

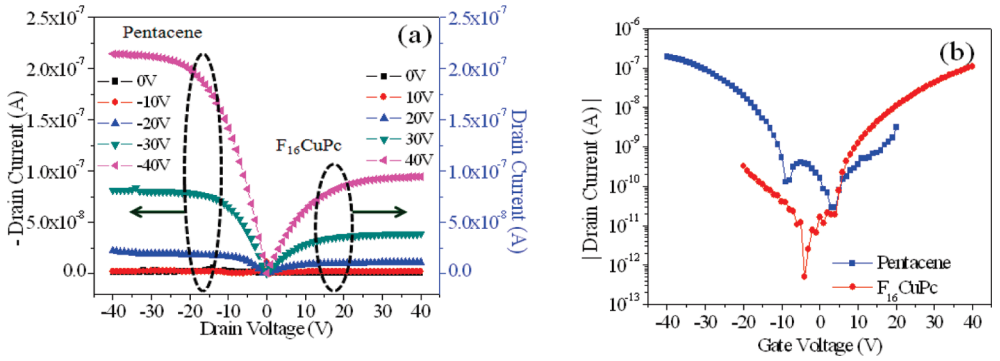


**Figure 2.** (a) Output characteristic curves of the *p*-channel OTFT (*L*: 250 $\mu$m, *W*: 200 $\mu$m) and the *n*-channel OTFT (*L*: 50 $\mu$m, *W*: 4,000 $\mu$m) in a complementary inverter and (b) the OTFTs' corresponding transfer characteristic curves without illumination measured at $V_{ds}$ = 40 V (*n*-channel) and $V_{ds}$ = −40 V (*p*-channel) in air.

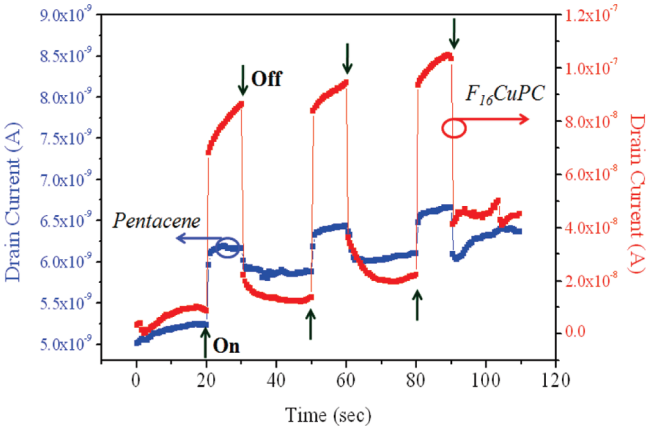


**Figure 3.** Dynamic photoresponses of the pentacene and F16CuPc OTFTs with respect to illumination. The light pulses were turned on for 10 s and off for 20 s. $V_{ds}$ and $V_{gs}$ were fixed at −10 V (for the pentacene OTFT) and +10 V (for the F16CuPc OTFT) throughout the measurement.

Each photoresponse cycle consisted of four transient regimes: a sharp rise, steady state, and sharp decay, followed by the slow relaxation of the drain current. During illumination, the current remained steady and stable with slight current increase, commonly observed in OPTs.[16,25,26] The current ratio between under illumination and in dark ($I_{light}/I_{dark}$) were calculated to be about 9.92 and 1.12 for the F16CuPC (*L*: 50 $\mu$m, *W*: 4,000 $\mu$m) and the pentacene OTFTs (*L*: 250 $\mu$m, *W*: 200 $\mu$m), respectively by comparing the current under illumination and in dark of the first current cycle in Figure 3. In order to investigate size effect of OTFTs on the photoresponse behavior, we have fabricated pentacene OTFT (*L*: 50 $\mu$m, *W*: 4,000 $\mu$m) with the same dimension as F16CuPc OTFT. The current ratio ($I_{light}/I_{dark}$) of the device was calculated to be about 1.59 indicating that although there is some size effect, the different photoresponse behavior from F16CuPc OTFT might be more affected by the intrinsic properties of the materials. In general, as the characteristic of phototransistor depends on the number of photogenerated charge carriers in the channel region of OTFT, the amount of light absorbed by the material is critical issue. When the light with photon energy equal to and higher band gap, a number of excitons are generated in the channel region, that is, the electrons from highest occupied molecular orbital (HOMO) of the material will be excited to the lowest unoccupied molecular orbital (LUMO) of the material resulting in increase in charge carrier concentration in the channel region and hence increase the current of the device.[23] It is found from literature that the bandgap of F16CuPc and pentacene is in the range of 1.4−1.6 eV[23] and 1.85−1.9 eV,[27] respectively. The bandgap of F16CuPc is smaller than that of pentacene, indicating that F16CuPc molecules might be more easily excited by the visible light. In addition, it is also found that the F16CuPc has a wide absorption range than any other materials.[23,28] But, as the device performance can also be affected by the exciton dissociation, diffusion and transport of the charge carriers inside the materials to the external electrodes, more studies are necessary for clear understanding on this matter. Based on the results in Figure 3, we expect that under the same light intensity more charge carriers can be generated in F16CuPC than pentacene, and the current in F16CuPc OTFT will increase more than pentacene, indicating that when the circuit comprising of F16CuPc and pentacene OTFT is exposed to light, its performance can be controlled by the illumination.

The output (measured at $V_{gs}$ = 40 V) (Figure 4a) and transfer (measured at $V_{ds}$ = 30 V) (Figure 4b) characteristics of the F16CuPC OTFT with respect to illumination show that with increasing incident light intensity, the drain current gradually increased due to the increase of photogenerated charge carriers (Figure 4). Under illumination, $I_{ds}$ increased and $V_{th}$ decreased compared with the values under the same $V_{gs}$ without illumination. This indicates that the device can be switched on by illumination at reduced voltage due to the photogenerated charge carriers in the device's channel region. The current ratio between under illumination and in dark ($I_{light}/I_{dark}$) is higher in the depletion region, in which there are no electric-field induced charge carriers, than in the accumulated region, since the characteristics of the device in the accumulated region are mainly dominated by field-induced charge carriers. As shown in Figure 4, after turning off the light, $I_{ds}$ decayed rapidly to a certain level (metastable) (solid line) because of the recombination of proximal carriers and trapped charges screen the gate voltage leading to a higher current compared to that in the dark (solid square).[18,29,30] The observed phenomenon, referred to as persistent conductivity, has been previously observed in organic thin film devices, which is imputed to the slow recombination of induced electrons and holes. It is also observed in phototransistors when no gate voltage is applied, and can remains for hours.[30,31] The same system has been reported in our previous communications by comparing examining the interface/surface properties of different gate dielectric.[15,16] It was found that the persistent conductivity can be reduced by designing optimum interface between gate

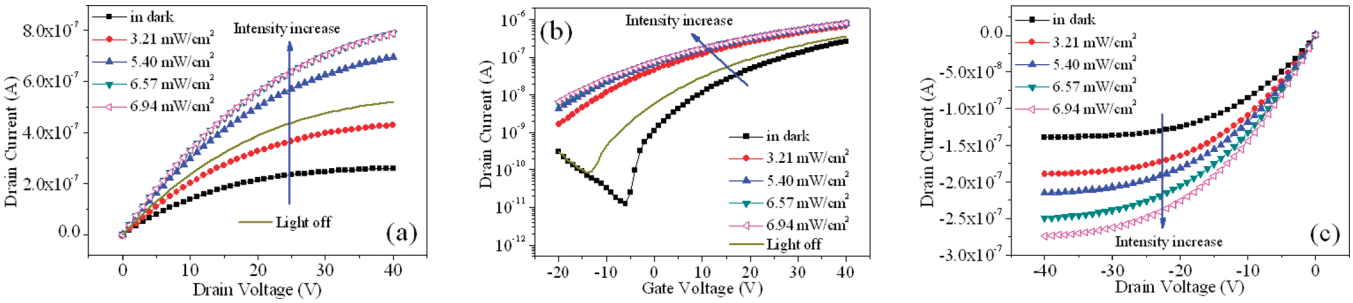


**Figure 4.** (a) Output characteristic curves of the F16CuPc OTFT measured at $V_{gs}$ = 40 V in dark and under illumination with different optical power, and (b) corresponding transfer characteristic curves measured at $V_{ds}$ = 30 V in dark and under illumination with different optical power. Solid line of a and b represents current response right after turning off the light. (c) Output characteristic curves of the pentacene OTFT measured at $V_{gs}$ = −40 V in dark and under illumination with different optical power.

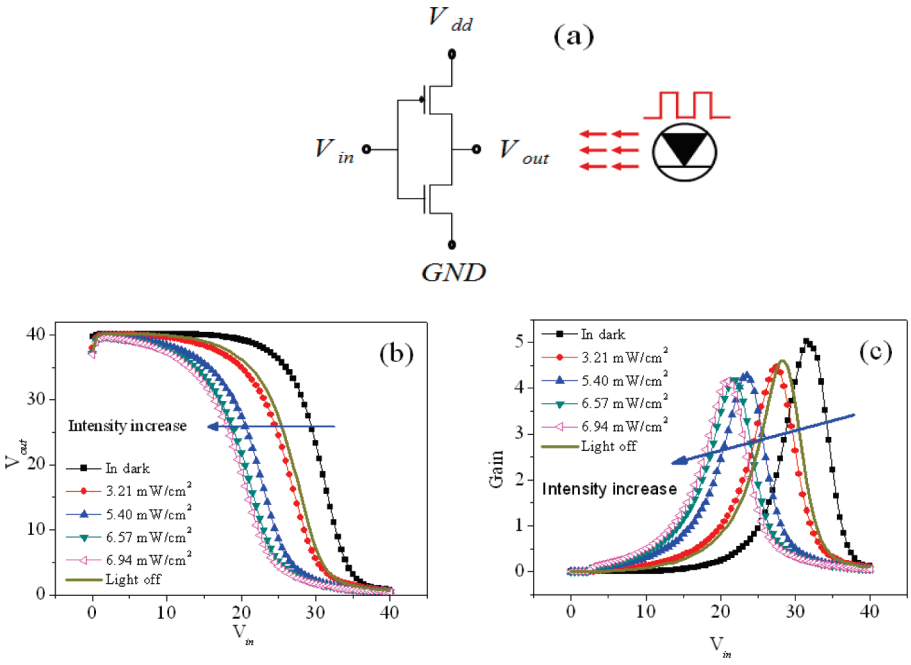


**Figure 5.** (a) Circuit diagram of the complementary inverter. (b) Voltage transfer ($V_{out}$−$V_{in}$) characteristic curve (VTC) and (c) voltage gain of the complementary inverter at a supply voltage ($V_{dd}$) of 40 V and various incident light intensities. Solid line of each figure represents current response right after turning off the light.

dielectric and organic semiconductor. The output (measured at $V_{gs}$ = −40 V) characteristics of the pentacene OTFT with respect to illumination was also shown in Figure 4c and the characteristic is also in similar trend to F16CuPC OTFT.

The effect of incident light intensity on the electrical characteristics of the complementary inverter was studied by measuring photoresponse of the circuit with respect to illumination intensity. Figure 5 shows the voltage transfer characteristic ($V_{out}$−$V_{in}$) curve (VTC) of the complementary inverter at a supply voltage ($V_{dd}$) of 40 V and various incident light intensities. Without light illumination the logic threshold voltage ($V_M$) was 28.6 V and the maximum voltage gain ($\delta V_{out}/\delta V_{in}$) ($A_v$) was 5.02, obtained at $V_{in}$ = 28.6 V. The logic threshold voltage ($V_M$) of the complementary inverter was greater than $V_{dd}/2$ = 20 V because of the difference of electrical performances between the pentacene and F16CuPC OTFTs.[32] With increasing light power, $V_M$ decreased up to 19.9 V at an optical input power of 6.94 mW/cm$^2$, almost equal to $V_{dd}/2$.

**Table 1. Summary of $V_M$ and Gain of the Complementary Inverter as a Function of Light Intensity**

| intensity (mW/cm$^2$) | 0 | 3.21 | 5.40 | 6.57 | 6.94 | 0[a] |
|---|---|---|---|---|---|---|
| $V_M$ | 28.6 | 24.9 | 21.8 | 20.5 | 19.9 | 25.6 |
| gain | 5.02 | 4.47 | 4.29 | 4.19 | 4.16 | 4.39 |

[a] Measured right after turning off the light.

The reduction of $V_M$ to almost $V_{dd}/2$ is likely because of the increase of current of the F16CuPC OTFT to the level of the pentacene OTFT by the increase of photogenerated charge carriers under illumination. But, the voltage gain ($A_v$) was slightly decreased from 5.02 to 4.16. The $A_v$ of complementary inverter is expressed as follows:[33]

$$A_v = -(g_{mn} + g_{mp})/(g_{dn} + g_{dp}) = -(g_{mn} + g_{mp})/(r_{on}||r_{op})$$

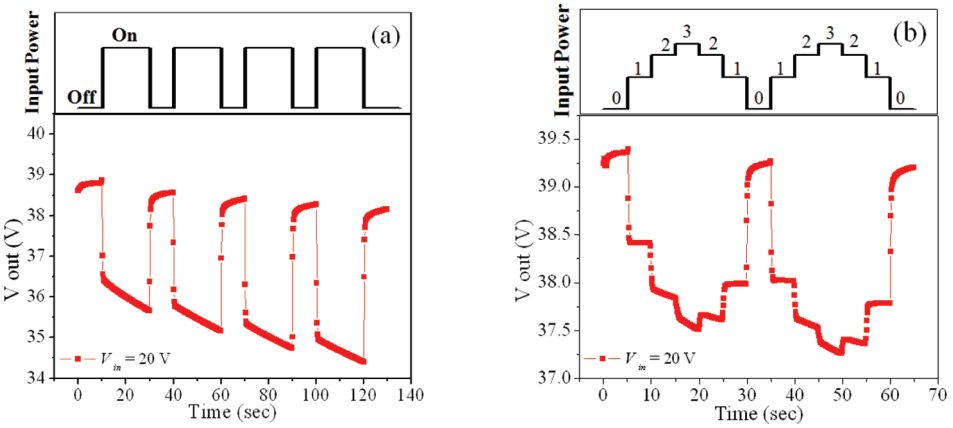


**Figure 6.** (a) Dynamic photoresponse of the complementary inverter, measured at a fixed $V_{dd}$ = 40 V and fixed $V_{in}$ = 20 V. Light of optical power 6.94 mW/cm$^2$ was turned on for 10 s and off for 20 s. (b) Multilevel light sensing in the complementary inverter, measured at fixed $V_{dd}$ = 40 V and $V_{in}$ = 20 V. Top and bottom panels depict the level of light intensity and the inverter's dynamic photoresponse, respectively. The four light intensities used were 0 (in dark, state 0), 3.21 (state 1), 5.40 (state 2), and 6.57 mW/cm$^2$ (state 3) with switching between them every 5 s.

where

$$g_{mn} = (\partial I_{ds}/\partial V_{gs})_{n\text{-channel}}, g_{mp} = (\partial I_{ds}/\partial V_{gs})_{p\text{-channel}},$$

$$g_{dn} = (\partial I_{ds}/\partial V_{ds})_{n\text{-channel}} = r_{on}{}^{-1},$$

$$g_{dp} = (\partial I_{ds}/\partial V_{ds})_{p\text{-channel}} = r_{op}{}^{-1}$$

Although $g_{mn}$ and $g_{mp}$ increase by illumination, that is, $I_{ds}$ of F16CuPc OTFT and pentacene OTFT increase, $g_{dn}$ and $g_{dp}$ also increase as shown in Figure 4. Therefore undoubtedly $A_v$ decreased slightly because $g_{dn}$ and $g_{dp}$ increased more than $g_{mn}$ and $g_{mp}$ with increasing the light intensity. Immediately after turning off the light, we observed that the VTC curve is not the same as that observed in the pristine device in dark, ascribable to the persistent current, as observed in Figure 4. The $V_M$ and $A_v$ of the complementary inverter as a function of light intensity are summarized in Table 1. The results in Figure 5 suggest that optical signal could effectively control the performance complementary inverter, that is, by applying an appropriate bias to the inverter, it can switch from high $V_{out}$ to low $V_{out}$ once it detects light with the threshold power.

To investigate the dynamic photoresponse of the complementary inverter, $V_{out}$ was measured as a function of time with fixed $V_{in}$ (constant) and light intensity (constant) during repeated switching of the light as shown in Figure 6a. The photoresponse of the inverter was measured at a fixed $V_{dd}$ = 40 V and $V_{in}$ = 20 V. The light pulse (top panel of Figure 6a) was generated by switching the light with optical power 6.94 mW/cm$^2$ on for 20 s and off for 10 s. The measured dynamic photoresponse behavior of the inverter clearly indicates that a light can be an additional control parameter for the inverter and it can function as a switch. Each photoresponse cycle had three transient regimes: rise, steady state with persistent conductivity and decay. Immediately after the light was turned on, $V_{out}$ drop was observed and back to almost the original value observed when the light was turned off. This was due to the more increased current of the n-channel OTFT caused by photogenerated charge carriers and again demonstrates the device's suitability as an optoelectronic switch. The gradual decrease of $V_{out}$ with time in the steady state was observed while the light was on, possibly because of the increase of current with time (persistent current) while the light was on, as observed in Figure 3. However, this kind of gradual increase of current and subsequently decrease of $V_{out}$ could be reduced through the optimization of device structure, such as improving the interface between the gate dielectric and semiconductor.

Finally, circuits could rely on varying light intensities, rather than being restricted to binary states of on or off. With different light intensities, the inverter can be precisely controlled and it can sense light with different intensity, multilevel light sensing (Figure 6b). To realize that multilevel light sensing in the complementary inverter, photoresponses were measured under illumination of four repeatedly cycled intensities. Dynamic multilevel light sensing was measured at fixed $V_{dd}$ = 40 V and $V_{in}$ = 20 V. The top panel of Figure 6b depicts the level of light intensity and the bottom shows the dynamic photoresponse of the inverter. The four different light intensities were: 0 mW/cm$^2$ (in dark, state 0), 3.21 mW/cm$^2$ (state 1), 5.40 mW/cm$^2$ (state 2) and 6.57 mW/cm$^2$ (state 3). Switching between intensities occurred every 5 s. The dynamic photoresponse of the circuit mirrored that of the input optical pulse, as shown in the figure; as light intensity increased or decreased, $V_{out}$ similarly, but oppositely, decreased or increased, indicating that the inverter can function as a multilevel light sensor. The figure also indicates that many more level can be created by optimizing the operation conditions, which could give more flexibility to the operation and design of multifunctional organic devices. Here, it is worthwhile to mention that the $V_{out}$ value from dynamic photoresponse measurement is a little different from that of Figure 3 because the devices were not the same. Furthermore it indicates that more optimization might be necessary for the high performance device. These results suggest the possibility of electronic circuits that can detect light's wavelength through the number of photogenerated charge carriers, as this strongly depends on the wavelength (photon energy) of the light. These results indicate that the device can efficiently be used as an element in most forms of complicated circuits including electro-optical transceivers and full color imaging sensor arrays.

## CONCLUSIONS

A photosensitive organic-based complementary inverter was fabricated by integrating *p*-channel (pentacene) and *n*-channel (F16CuPc) OTFTs with polymeric gate dielectric. The OTFTs

in the circuit showed typical *n*- and *p*-channel characteristics, with the n-channel (F16CuPc) OTFT showing a more sensitive photoresponse behavior than the p-channel (pentacene) OTFT. The characteristics of the organic circuit were controlled by the incident light intensity, a gate bias, or both. The logic threshold ($V_M$, $V_{in} = V_{out}$) was reduced from 28.6 V without illumination to 19.9 V at 6.94 mW/cm$^2$. By using optical or combined optical and electrical pulse signals, multilevel light sensing of the inverter was investigated through measurement of its dynamic photoresponses. The circuit displayed potential to be used in various optoelectronic applications including optical sensors, photodetectors and electro-optical transceivers.

## AUTHOR INFORMATION

### Corresponding Author

*Tel: +82 2 450 3397. Fax: +82 2 3436 5382. E-mail: pyosm@konkuk.ac.kr.

## ACKNOWLEDGMENT

This work was supported by the National Research Foundation (NRF) through EPB Center (R11-2008-052-03003).

## REFERENCES

(1) Oritz, R. P.; Facchetti, A.; Marks, T. J. *Chem. Rev.* **2010**, *110*, 205–239.

(2) (a) Virkar, A.; Mannsfeld, S.; Oh, J. H.; Toney, M. F.; Tan, Y. H.; Liu, G.; Scott, C.; Miller, R.; Bao, Z. *Adv. Func. Mater.* **2009**, *19*, 1962–1970. (b) Tan, H. S.; Mathews, N.; Cahyadi, T.; Zhu, F. R.; Mhaisalkar, S. G. *Appl. Phys. Lett.* **2009**, *94*, 263303.

(3) Hong, J.; Lee, S. *Angew. Chem., Int. Ed.* **2009**, *48*, 3096–3098.

(4) Dhagat, P.; Haverinen, H. M.; Kline, R. J.; Jung, Y.; Frscher, D. A.; DeLongchamp, D. M.; Jabbour, G. E. *Adv. Funct. Mater.* **2009**, *19*, 2365–2372.

(5) Wang, H.; Wen, Y.; Yang, X.; Wang, Y.; Zhou, W.; Zhang, S.; Zhan, X.; Liu, Y.; Shui, Z.; Zhu, D. *ACS Appl. Mater. Interfaces* **2009**, *1*, 1122–1129.

(6) Oh, Y.; Pyo, S.; Yi, M.; Kwon, S. *Org. Electron.* **2006**, *7*, 77–84.

(7) Bao, Z.; Lovinger, A.; Brown, J. *J. Am. Chem. Soc.* **1998**, *120*, 207–208.

(8) Tatemichi, S.; Ichikawa, M.; Kato, S.; Koyama, T.; Taniguchi, Y. *Phys. Stat. Sol. (RRL)* **2008**, *2*, 47–49.

(9) Tang, Q.; Tong, Y.; Hu, W.; Wan, Q.; Bjornholm, T. *Adv. Mater.* **2009**, *21*, 4234–4237.

(10) Briseno, A. L.; Mannsfeld, S. C. B.; Reese, C.; Hancock, J. M.; Xiong, Y.; Jenekhe, S. A.; Bao, Z.; Xia, Y. *Nano Lett.* **2007**, *7*, 2847–2853.

(11) Kitamura, M.; Arakawa, Y. *Appl. Phys. Lett.* **2007**, *91*, 053505.

(12) (a) Ling, M.; Bao, Z.; Erk, P.; Koenemann, M.; Gomez, M. *Appl. Phys. Lett.* **2007**, *90*, 093508. (b) Tan, H. S.; Wang, B. C.; Kamath, S.; Chua, J.; Shojaei-Baghini, M.; Rao, V. R.; Mathews, N.; Mhaisalkar, S. G. *IEEE Electron Device Lett.* **2010**, *31*, 1311–1313.

(13) Chen, H.; Hou, J.; Zhang, S.; Liang, Y.; Yang, G.; Yang, Y.; Yu, L.; Wu, Y.; Li, G. *Nat. Photonics* **2009**, *3*, 649–653.

(14) Png, R.; Chia, P.; Tang, J.; Liu, B.; Sivaramakrishnan, S.; Zhou, M.; Khong, S.; Chan, H. S. O.; Burroughes, J. H.; Chua, L.; Friend, R. H.; Ho, P. K. H. *Nat. Mater.* **2010**, *9*, 152–158.

(15) Mukherjee, B.; Mukherjee, M.; Choi, Y.; Pyo, S. *J. Phys. Chem. C.* **2009**, *113*, 18870–18873.

(16) Mukherjee, B.; Mukherjee, M.; Choi, Y.; Pyo, S. *ACS Appl. Mater. Interfaces* **2010**, *2*, 1614–1620.

(17) Saragi, T. P.; Pudzich, R.; Fuhrmann-Lieker, T.; Salbeck *J. Appl. Phys. Lett.* **2004**, *84*, 2334–2336.

(18) Narayan, K. S.; Kumar, N. *Appl. Phys. Lett.* **2001**, *79*, 1891–1893.

(19) Marjanovic, N.; Singh, T. B.; Dennler, G.; Gunes, S.; Neugebauer, H.; Sariciftci, N. S.; Schwodiauer, R.; Bauer, S. *Org. Electron.* **2006**, *7*, 188–194.

(20) (a) Jiang, H.; Yang, X.; Cui, Z.; Liu, Y.; Li, H.; Hu, W. *Appl. Phys. Lett.* **2009**, *94*, 123308. (b) Noh, Y.; Kim, D; Yoshida, Y.; Yase, K.; Jung, B.; Lim, E.; Shim, H. *Appl. Phys. Lett.* **2005**, *86*, 043501. (c) Pal, T.; Khondaker, S. I. *Nanotechnology* **2010**, *21*, 325201. (d) Guo, Y.; Du, C.; Di, C.; Zheng, J.; Sun, X.; Wen, Y.; Zhang, L.; Wu, W.; Yu, G.; Liu, Y. *Appl. Phys. Lett.* **2009**, *94*, 143303.

(21) Labram, J. G.; Wobkenberg, P. H.; Bradley, D. D. C.; Anthopoulos, T. D. *Org. Electron.* **2010**, *11*, 1250–1254.

(22) Anthopoulos, T. D. *Appl. Phys. Lett.* **2007**, *91*, 113513.

(23) Tang, Q.; Li, L.; Song, Y.; Liu, Y.; Li, H.; Xu, W.; Liu, Y.; Hu, W.; Zhu, D. *Adv. Mater.* **2007**, *19*, 2624–2628.

(24) (a) Kwon, J.; Chung, M.; Oh, T.; Bae, H.; Park, J.; Ju, B.; Yakuphanoglu, F. *Sensor Actuat. A* **2009**, *156*, 312–316. (b) Okur, S.; Yakuphanoglu, F.; Stathatos, E. *Microelectron. Eng.* **2010**, *87*, 635–640. (c) Hu, Y; Dong, L.; Wang, L.; Qiu, Y. *J. Appl. Phys. Lett.* **2006**, *45*, L96–L98.

(25) Chuang, C. S.; Chen, F. C.; Shieh, H. P. D. *Org. Electron.* **2007**, *8*, 767–772.

(26) Jung, T.; Dodabalapur, A.; Wenz, R.; Mohapatra, S. *Appl. Phys. Lett.* **2005**, *87*, 182109.

(27) Choi, J.; Hwang, D.; Hwang, J.; Kim, J.; Im, S. *Appl. Phys. Lett.* **2007**, *90*, 113515.

(28) Optiz, A.; Wagner, J.; Brutting, W.; Salzmann, I.; Koch, N.; Manara, J.; Pflaum, J.; Hinderhofer, A.; Schreiber, F. *IEEE J. Sel. Top. Quantum Electron.* **2010**, *16*, 1707–1717.

(29) Dutta, S.; Narayan, K. S. *Adv. Mater.* **2004**, *16*, 2151–2155.

(30) Mas-Torrent, M.; Hadley, P.; Crivillers, N.; Veciana, J.; Rovira, C. *ChemPhysChem* **2006**, *7*, 86–88.

(31) Lutsykm, P.; Janus, K.; Mikolajczyk, M.; Sworakowski, J.; Boratynski, B.; Tlaczala, M. *Org. Electron.* **2010**, *11*, 490–497.

(32) Ng, T.; Sambandan, S.; Lujan, R.; Arias, A.; Newman, C. R.; Yan, H.; Facchetti, A. *Appl. Phys. Lett.* **2009**, *94*, 233307.

(33) Allen, P. E.; Holberg, D. R. *CMOS Analog Circuit Design*; Oxford University Press: Oxford, U.K., 1987; p 269.